crystals

MDPI

Article

Enhanced Thermal Stability in Cu1234 Superconductor with Oxygen Annealing

Luchuan Shi [1,2,†], Kai Huang [1,2,†], Haoyu Zheng [1,3], Xiaoming Chen [1,3], Yuling Dai [1,4], Yi Peng [1,2], Jianfa Zhao [1,*], Xiancheng Wang [1,2,*] and Changqing Jin [1,2,*]

[1] Beijing National Laboratory for Condensed Matter Physics, Institute of Physics, Chinese Academy of Sciences, Beijing 100190, China; shiluchuan15@iphy.ac.cn (L.S.); huangkai@iphy.ac.cn (K.H.); userzhy0123@163.com (H.Z.); xiaomingchen2025@163.com (X.C.); 18297903640@163.com (Y.D.); ypeng@iphy.ac.cn (Y.P.)
[2] School of Physics, University of Chinese Academy of Sciences, Beijing 100190, China
[3] School of Material Science and Engineering, Henan University of Technology, Zhengzhou 450001, China
[4] School of Chemistry and Chemical Engineering, Xi'an University of Architecture and Technology, Xi'an 710311, China
* Correspondence: zhaojf@iphy.ac.cn (J.Z.); wangxiancheng@aphy.iphy.ac.cn (X.W.); jin@iphy.ac.cn (C.J.)
† These authors contributed equally to this work.

Abstract

Recently, $CuBa_2Ca_3Cu_4O_{10+\delta}$ (Cu1234) has garnered significant interest owing to its distinctive triple-high superconducting properties (118K high T_c, combined with high J_c and high H_{irr} at liquid nitrogen temperature at ambient pressure) and potential for practical applications. The Cu1234 is initially synthesized at high pressures and is stable at a room temperature range but tends to decompose upon heating above 300 °C at ambient. In this study, we investigate the thermal stability of Cu1234 through annealing at various temperatures and oxygen pressures. It is found that Cu1234 starts to decompose at approximately 350 °C, 550 °C, and 600 °C when annealed at 1 bar, 100 bar, and 150 bar oxygen pressure, respectively. Prior to decomposition, however, the superconducting properties remain largely unchanged. The decrease in oxygen occupancy within the BaO layer of the $BaCuO_{3-\delta}$ charge reservoir block is proposed to be the primary cause of the structural instability of Cu1234, while higher oxygen pressures retard oxygen loss from this block. Our result suggests that the decomposition temperature of Cu1234 will further increase with higher oxygen pressure, e.g., possibly to 800 °C at 260 bar if a linear extrapolation is adopted. This study offers important insights for fabricating Cu1234 tapes via the powder-in-tube method.

Keywords: Cu1234; oxygen annealing; thermal stability

Academic Editor: Andrei Vladimirovich Shevelkov

Received: 30 January 2026
Revised: 28 March 2026
Accepted: 8 April 2026
Published: 13 April 2026

1. Introduction

$CuBa_2Ca_3Cu_4O_{10+\delta}$ (Cu1234), discovered as a high-temperature superconductor with a T_c of ~118 K, has recently attracted renewed interest because of its promising practical applications owing to its triple-high properties [1,2]. It has been revealed that Cu1234 has high T_c, high critical current density J_c (~5×10^5 A/cm^2 at self-field) and high irreversible field H_{irr} (>20 Tesla) in the liquid nitrogen temperature range [3–5], exhibiting overall performance superior to that of the established superconducting tapes of $Bi_2Sr_2Ca_2Cu_3O_x$ (Bi2223) and $YBa_2Cu_3O_{7-\delta}$ (YBCO) [6,7]. The triple-high properties are attributed to the small anisotropy factor of Cu1234 similar to YBCO [8,9]. Following the method of manufacture of the YBCO tape in the form of epitaxial thin-films, the Cu1234 and its related phase

$CuBa_2Ca_2Cu_3O_{8+\delta}$ (Cu1223) films have been successfully grown on different single-crystal substrates and flexible Hastelloy tapes [10,11]. It was found that a partially incorporated carbon element at the [CuO_2] deficient charge reservoir layer resembling the tetragonal phase of YBCO is relatively easier to synthesize the Cu1234 structure at high pressure. The superconductor is consequently sometime labeled as (Cu,C)1234 [12,13]. To fabricate a Cu1234 tape, the epitaxial thin-film approach seems feasible [14–16], but the powder-in-tube (PIT) method poses a significant challenge. The PIT process, used for Bi2223/Ag tapes, involves intermediate rolling and requires high-temperature healing of cracks at ambient pressure to enhance superconducting connectivity [17,18]. However, bulk polycrystalline Cu1234 can only be synthesized under high-pressure conditions. Therefore, if the PIT method is adopted for Cu1234 tapes manufacture, a critical issue must be addressed: how to heat-treat the samples to heal the cracks without degrading their superconducting properties at ambient pressure or available pressures.

In this work, we systematically investigate the thermal stability and the evolution of the superconducting properties of Cu1234 by annealing the sample at varying temperature and different atmospheres: 1 bar O_2, 100 bar O_2 and 150 bar O_2. It is found that the structure of Cu1234 begins to decompose at about 350 °C in 1 bar O_2 due to the oxygen loss from the $BaCuO_{3-\delta}$ charge reservoir block during the annealing process, and high oxygen pressure can efficiently slow down the oxygen loss and enhance the decomposition temperature. Our result suggests that the decomposition temperature of Cu1234 will further increase with higher oxygen pressure, e.g., possibly to 800 °C at 260 bar if a linear extrapolation is adopted. At this temperature, cracks and grain boundaries could be effectively healed, thereby enhancing the superconducting connectivity—a process similar to observations in $Bi_2Sr_2Ca_2Cu_3O_x$ tapes. This study therefore provides important insights for fabricating Cu1234 tapes via the PIT method.

2. Materials and Methods

The polycrystalline Cu1234 sample was synthesized by a solid-state reaction method under high pressure and high temperature conditions. The synthesis procedure followed established methods described in the literature [1,2]. Cu1234 samples were annealed in a high-pressure tube furnace for 12 h at various temperatures under three different atmospheres: 1 bar O_2, 100 bar O_2 or 150 bar O_2 air. Samples were heated at 5 °C/min to the target temperature, held for 12 h, and then cooled at 5 °C/min. DC magnetic susceptibility measurements were performed using a Magnetic Property Measurement System (Quantum Design MPMS3) at the Institute of Physics, Chinese Academy of Siences (IoPCAS) in Beijing, China with an applied magnetic field of 30 Oe under both zero-field-cooled (ZFC) and field-cooled (FC) modes. All samples were cut into identical rectangular dimensions of approximately $3 \times 2 \times 2$ mm^3 to ensure consistent demagnetizing factors, allowing direct comparison of relative SVF values without explicit demagnetization corrections. The superconducting volume fraction was estimated using the relation SVF = $-4\pi\chi$, where χ is the DC magnetic susceptibility in emu/cm^3·Oe at 5 K under ZFC conditions. T_c is defined as the temperature at which the magnetic susceptibility becomes negative, i.e., the onset of the diamagnetic signal corresponding to the superconducting transition. Phase composition and structural changes after annealing were examined by X-ray diffraction (XRD) with a Philips X'pert diffractometer using a Huber diffractometer with Cu $K_{\alpha 1}$ radiation (λ = 1.5406 Å, 40 kV, 30 mA) at the IoPCAS in Beijing China. Diffraction patterns were collected over the 2θ range of 10–100° with a step size of 0.005°. Rietveld refinement of the XRD data was carried out using the GSAS program with version of v1.80 [19].

3. Results and Discussions

Figure 1 shows the crystal structure of Cu1234, which consists of superconducting layers [$Ca_3Cu_4O_8$] (SCL) with four CuO_2 planes and a charge-reservoir block (CRB) $BaCuO_{3-\delta}$. The CuO_6 octahedra within the CRB are compressed. This compression lifts the energy of the Cu-3dz^2 orbital, thereby enhancing conductivity along the *c*-axis and strengthening the coupling between SCL. Consequently, the system exhibits a small superconducting anisotropy [9]. Furthermore, the oxygen sites in the CRB are only partially occupied, with the occupancy determining the hole carrier density. A superstructure with $a \times 2b \times 2c$ modulation has been observed due to the oxygen vacancy ordering [20]. The resulting 90° microdomains, where the *c*-axes are parallel while the *a*-axes are mutually perpendicular, can act as natural flux-pinning centers and contribute to the high J_c and high H_{irr} in Cu1234 [20].

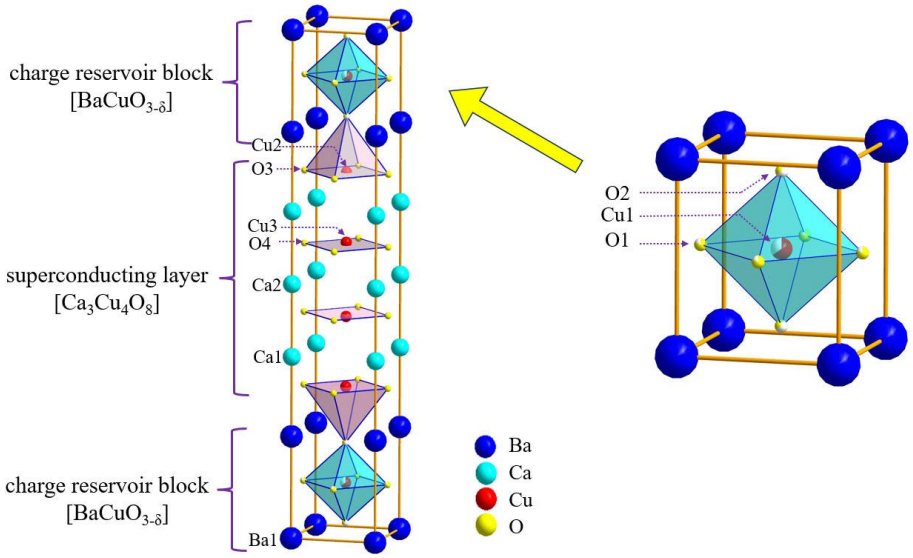

Figure 1. The schematic crystal structure of Cu1234 superconductor. The enlarged view (right figure) of the charge reservoir blocks of $BaCuO_{3-\delta}$ displays the partial occupation on the in-plane O1, apical O2 and Cu sites.

Figures 2a and S1 present the XRD patterns of the Cu1234 sample annealed at different temperatures under an oxygen pressure of 1 bar. At this pressure, no additional diffraction peaks appear below 350 °C. Above this temperature, however, weak peaks corresponding to $BaCuO_{2+x}$ (marked with *) emerge, indicating the onset of Cu1234 decomposition. The observed decomposition products, primarily $BaCuO_{2+x}$ and CuO, suggest that the initial stage of decomposition involves collapse of the charge reservoir block, releasing barium and copper to form binary oxides. A possible decomposition pathway is: $CuBa_2Ca_3Cu_4O_{10+\delta}$ $\rightarrow$ $BaCuO_{2+x}$ + CuO + ... Interestingly, even after heating to 450 °C, Cu1234 remains the dominant phase, suggesting relatively slow decomposition kinetics. The annealing behavior of Cu1234 was also investigated by M. Hirai et al. [21], who used a shorter heat treatment time (3 h above 400 °C) compared to ours (12 h). Their reported onset decomposition temperature (~450 °C) is higher than our observed value, likely due to the slow kinetics of the decomposition process [21]. The dependence of the apparent decomposition temperature on annealing duration suggests that the observed onset is at least partially kinetically controlled.

The lattice parameters (*a* and *c*) and unit-cell volume (*V*) of Cu1234, obtained from Rietveld refinement of the XRD data (see Figure S2), are plotted in Figure 2d as a function of annealing temperature. While the *a*-axis expands only slightly with increasing temperature, both the *c*-axis and the unit-cell volume increase noticeably above 300 °C. This expansion

is attributed to oxygen loss during annealing. The reduction in oxygen content lowers the average valence of Cu ions, increasing their ionic radius and thus causing an overall lattice expansion. A similar relationship between lattice parameters and oxygen content has been reported for the YBCO system [22,23].

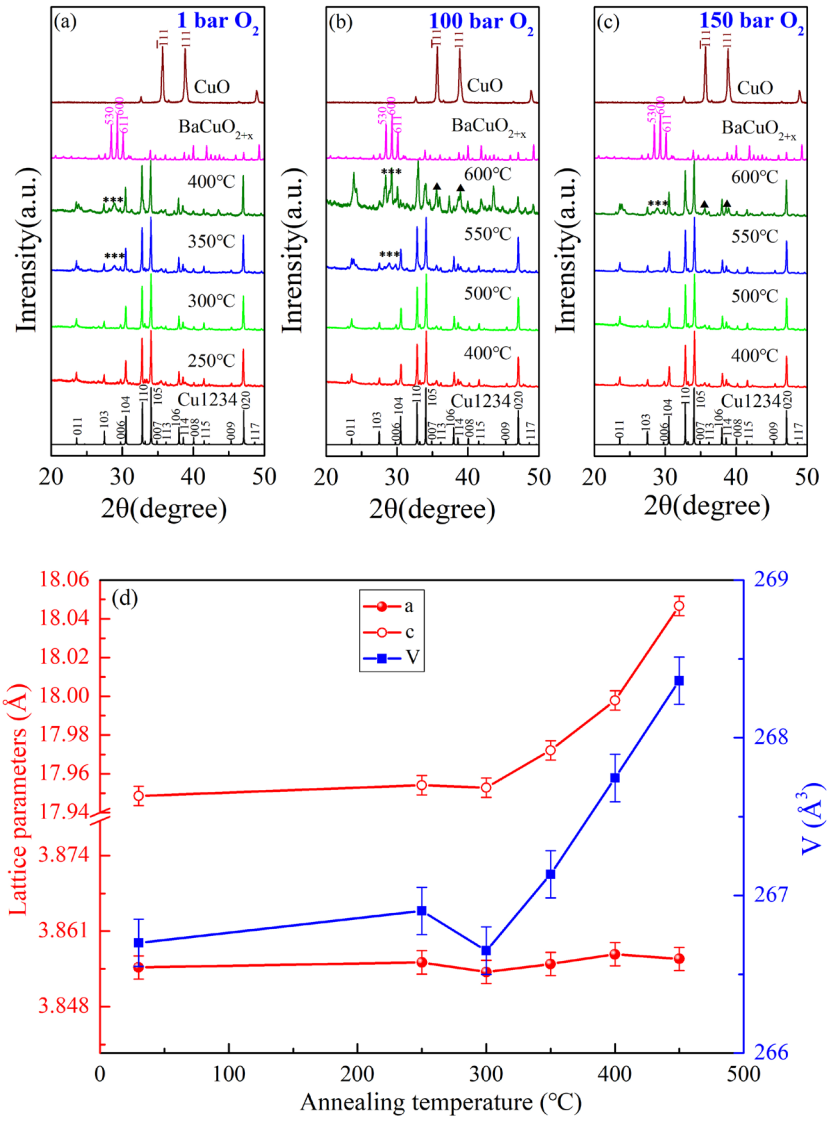

Figure 2. XRD patterns of Cu1234 sample annealed in (**a**) 1 bar, (**b**) 100 bar and (**c**) 150 bar oxygen pressure at different temperatures, respectively. For reference, standard XRD patterns of Cu1234, $BaCuO_{2+x}$, and CuO are also included in the figure. Peaks marked with an asterisk (*) and a triangle (▲) correspond to $BaCuO_{2+x}$ and CuO phases, respectively. (**d**) Evolution of lattice parameters for Cu1234 sample annealed at 1 bar oxygen pressure and different temperatures.

To investigate the effect of annealing on superconductivity, magnetic susceptibility measurements were performed. Figure 3a displays the zero-field-cooled (ZFC) magnetic susceptibility versus temperature for samples annealed at 1 bar O_2 and different temperatures. Both the T_c and the SVF vary systematically with increasing annealing temperature. Their trends are summarized in Figure 4a,b. For samples annealed below 300 °C in 1 bar O_2, T_c remains nearly constant, while the SVF decreases only slightly. The SVF stays above 70%, confirming that bulk superconductivity is preserved in Cu1234 under these conditions. As the annealing temperature is raised further, a step-like drop in T_c of more than 3 K occurs between 350 and 400 °C, accompanied by a substantial reduction in SVF to about 30%. At 450 °C, the SVF further decreases to approximately 5%. In cuprate superconductors, oxygen content is a key parameter

controlling T_c [24]. A well-known example is Cu1223, in which controlled deoxygenation via annealing in argon gradually increases T_c from 67 K to 118 K [25]. In contrast, the compound $CuBa_2Ca_4Cu_5O_{12+\delta}$ (Cu1245) shows a more complex evolution: with progressive oxygen loss, T_c first decreases slightly from 94.7 K to 93.3 K before rising to 99.0 K [26]. In the present case, the variation in T_c with annealing temperature at 1 bar O_2 is consistent with reported data from annealing under nitrogen flow and is attributed to the loss of lattice oxygen.

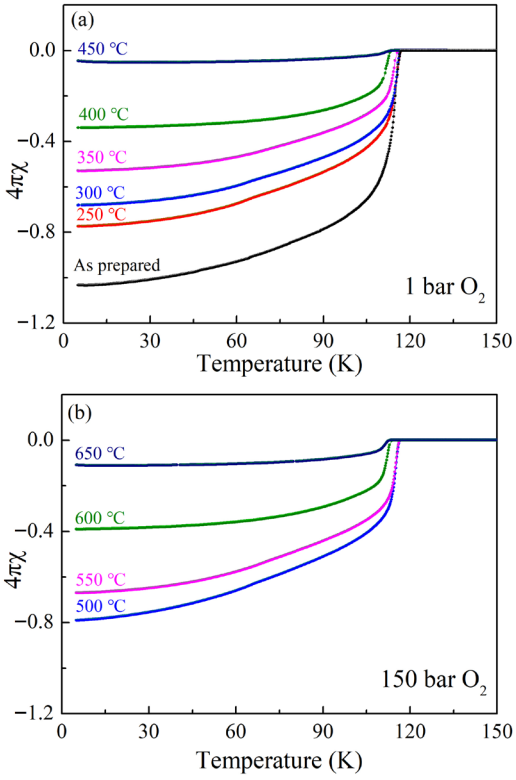

Figure 3. *M-T* curve measured with ZFC mode for Cu1234 superconductor annealed at different temperatures under (**a**) 1 bar O_2 and (**b**) 150 bar O_2.

Given the close relationship between structural stability, superconductivity, and oxygen loss, higher oxygen pressure is expected to retard oxygen loss during annealing. Accordingly, annealing experiments were performed under elevated oxygen pressures. Figure 2b,c show the XRD patterns of samples annealed at different temperatures under 100 bar and 150 bar O_2, respectively. Compared with annealing at 1 bar O_2, the onset decomposition temperature increases to approximately 550 °C at 100 bar O_2 and further rises to about 600 °C at 150 bar O_2. The enhanced thermal stability under high oxygen pressure is also reflected in the superconducting properties [27]. Figures 3b and 4a,b also present magnetic susceptibility and T_c as well as the SVF for the case of 150 bar O_2, respectively. Both the T_c and SVF curves obtained at 150 bar O_2 shift toward higher temperatures by roughly 200 °C relative to the results obtained at 1 bar O_2. These findings strongly indicate that high oxygen pressure effectively suppresses lattice oxygen loss during annealing, inhibits the decomposition of Cu1234, and thereby significantly improves the thermal stability of its superconducting state. In addition to suppressing oxygen loss from the charge reservoir block, high-pressure oxygen annealing may also induce microstructural changes such as grain growth, phase purification, and reduction in intergranular material. These effects are known to enhance superconducting connectivity in cuprate ceramics and may partially contribute to the retained superconducting volume fraction and stable T_c observed in samples annealed under elevated oxygen pressure. Further studies using electron microscopy are needed to decouple the contributions of oxygenation and microstructural evolution.

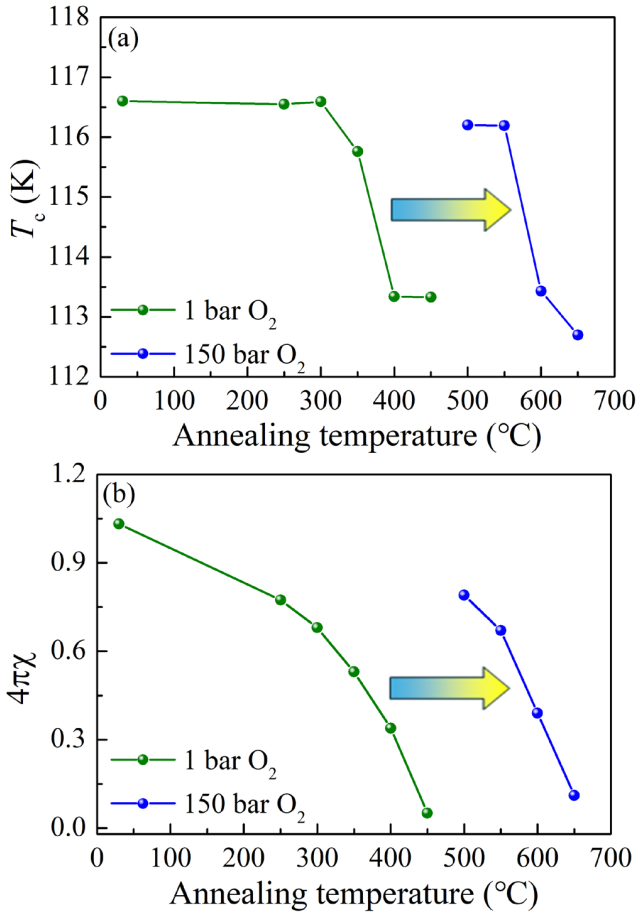

Figure 4. Evolution of (**a**) high critical temperature (T_c) and (**b**) superconducting volume fraction (SVF) of Cu1234 superconductor annealed in 1 bar O_2 and 150 bar O_2 with progressively increasing annealing temperature.

Figure 5 shows the relationship between oxygen pressure and decomposition temperature (T_d). Based on the limited data available, a linear fit of the three measured pressure points yields a slope of approximately 1.73 (±0.25) °C/bar. This trend suggests that the decomposition temperature of Cu1234 will further increase with higher oxygen pressure, e.g., possibly to 800 °C at 260 bar if a linear extrapolation is adopted.

A further notable finding is that oxygen loss during annealing primarily originates from a reduction in oxygen occupancy within the BaO layers of the $BaCuO_{3-\delta}$ CRB. The oxygen occupancy as a function of annealing temperature was examined through Rietveld refinement of XRD data from samples annealed at 1 bar O_2 with the refined results shown in Tables S1–S6. In the Rietveld refinement of the as-prepared Cu1234 sample, structural parameters were refined sequentially in the order of lattice parameters, peak profile parameters, atomic sites, thermal parameters, and occupancies. During occupancy refinement, the occupancies of metal sites were fixed to 1, while those of Cu1, O1, and O2 in the CRB were allowed to vary, based on previous reports indicating the presence of vacancies at these sites [28]. This yielded the initial structural model. For samples annealed at different temperatures (all XRD data collected at room temperature), this model was used as the starting point. Only lattice parameters, atomic sites, and the occupancies of O1 and O2 were refined. The occupancies of all metal sites (including Cu1) and thermal parameters were fixed to the values obtained from the unannealed sample, under the assumption that cation stoichiometry and thermal vibration behavior remain unchanged during low-temperature annealing. This refinement strategy minimized correlations between occupancy, scale factors, and thermal parameters, ensuring that the

observed variations in oxygen occupancy reliably reflect annealing-induced oxygen loss. Figure 6 displays oxygen occupancies in the $BaCuO_{3-\delta}$ CRB as a function of annealing temperature. O1 corresponds to oxygen in the CuO layers, and O2 corresponds to oxygen in the BaO layers. For the O2 site (BaO layer), the refined occupancy decreases from 0.81(9) (See Table S1) in the unannealed sample to 0.62(0) (See Table S6) after annealing at 450 °C under 1 bar O_2. The change of 0.19 is far larger than error values (~10^{-3}), demonstrating that this reduction is statistically significant and cannot be attributed to random refinement uncertainty. In contrast, the O1 site (CuO layer) shows occupancies from 0.27(6) (See Table S1) to 0.28(0) (See Table S6) across the same temperature range, with variations near to the error values. This confirms that oxygen loss occurs predominantly from the BaO layer, while the CuO layer remains stable. This indicates that oxygen in the BaO layers plays a decisive role in both superconductivity and thermal stability of Cu1234. Consequently, two approaches can be considered to control oxygen occupancy and enhance thermal stability: applying high oxygen pressure during annealing or doping Cu or Ba sites with higher-valence ions to intrinsically increase oxygen content. These strategies may also be combined, allowing effective superconducting connectivity to be achieved at lower oxygen pressures through higher annealing temperatures.

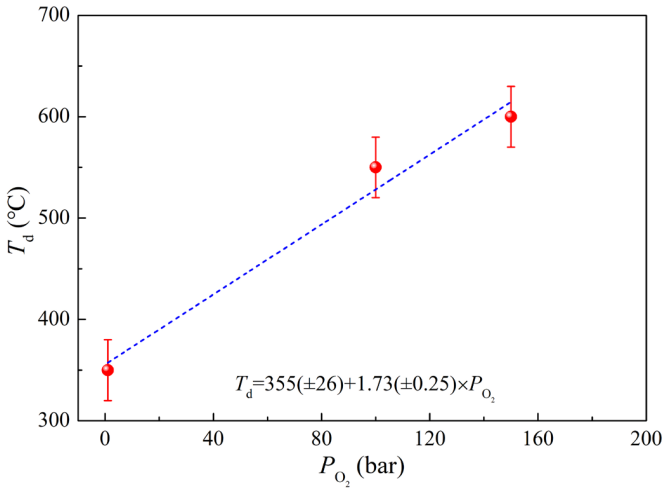

Figure 5. Evolution of the decomposition temperature (T_d) for Cu1234 superconductor as a function of external oxygen pressure P_{O2}. The red line represents the error bar, and the dashed blue line is the linear fit to the data.

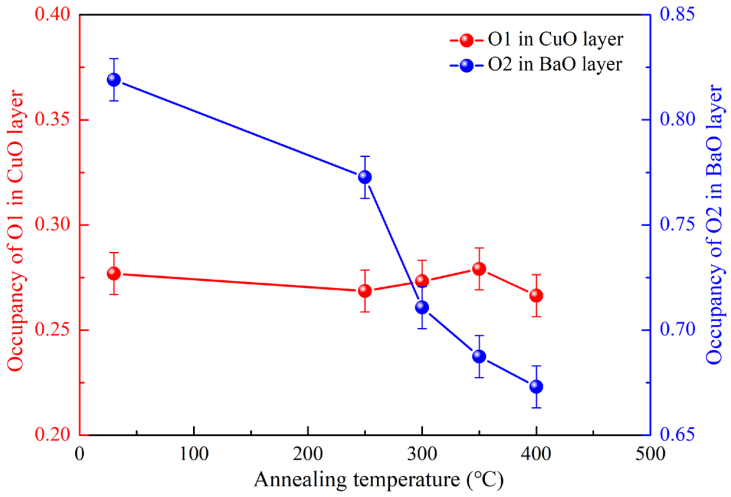

Figure 6. Oxygen occupancies in the $BaCuO_{3-\delta}$ charge reservoir block as a function of annealing temperature. O1 (red) corresponds to oxygen in the CuO layers, and O2 (blue) corresponds to oxygen in the BaO layers.

4. Conclusions

In summary, we have systematically examined the thermal stability of the Cu1234 superconductor through annealing under varying oxygen pressures. The onset decomposition temperature is found to be approximately 350 °C at 1 bar O_2 but increases to 600 °C under 150 bar O_2 while largely preserving superconducting properties. A clear linear correlation is observed between oxygen pressure and decomposition temperature, with a slope of about 1.73 (±0.25) °C/bar. Furthermore, refinement analysis suggests that the structural decomposition of Cu1234 is closely related to the reduction of oxygen occupancy within the BaO layers of the $BaCuO_{3-\delta}$ CRB. High oxygen pressure effectively suppresses this oxygen loss, thereby enhancing thermal stability. We note that this site-specific assignment currently relies on diffraction data alone and independent validation from complementary techniques such as TEM is desirable in future work. These findings offer valuable guidance for improving superconducting connectivity through annealing, particularly in the context of fabricating Cu1234 tapes using the PIT method.

Supplementary Materials: The following supporting information can be downloaded at: https://www.mdpi.com/article/10.3390/cryst16040261/s1, Figure S1: The XRD patterns of the Cu1234 samples annealed under an oxygen pressure of 1 bar; Figure S2: Rietveld refinement of the XRD data for Cu1234 samples annealed under an oxygen pressure of 1 bar; Tables S1–S6: Crystallographic Parameters of as prepared Cu1234 sample and samples annealed in 1 bar O_2 at different temperatures.

Author Contributions: Conceptualization, C.J.; methodology, L.S. and K.H.; validation, H.Z. and X.C.; investigation, Y.D. and Y.P.; writing—original draft preparation, J.Z.; writing—review and editing, X.W.; supervision, C.J. All authors have read and agreed to the published version of the manuscript.

Funding: This work was supported by the National Key Research and Development Program of China (Grant Nos. 2024YFA1408000, 2022YFA1403800, 2023YFA1406000), the CAS Superconducting Research Project (Grant No. SCZX-0101), the National Natural Science Foundation of China (Grant No. 12204515), and the Beijing Natural Science Foundation (Grant No. 1262041). J.Z. acknowledges the support of the Young Elite Scientists Sponsorship Program by CAST (Grant No. 2022QNRC001).

Data Availability Statement: Dataset available on request from the authors. The raw data supporting the conclusions of this article will be made available by the authors on request.

Conflicts of Interest: The authors declare no conflict of interest.

References

1. Jin, C.Q.; Adachi, S.; Wu, X.J.; Yamauchi, H.; Tanaka, S. 117 K Superconductivity in the Ba-Ca-Cu-O System. *Phys. C Supercond.* **1994**, *223*, 238–242. [CrossRef]
2. Jin, C.Q.; Adachi, S.; Wu, X.J.; Yamauchi, H. A new homologous series of compounds: Cu-12(n − 1)n:P. In *Advances in Superconductivity VII*; Springer: Tokyo, Japan, 1995; pp. 249–254.
3. Lynnyk, A.; Puzniak, R.; Shi, L.; Zhao, J.; Jin, C. Superconducting state properties of $CuBa_2Ca_3Cu_4O_{10+\delta}$. *Materials* **2023**, *16*, 5111. [CrossRef]
4. Campi, G.; Catricalà, M.; Chita, G.; Barba, L.; Shi, L.; Zhao, J.; Jin, C.; Bianconi, A. Lattice quantum geometry controlling 118 K multigap superconductivity in heavily overdoped $CuBa_2Ca_3Cu_4O_{10+\delta}$. *Phys. Rev. Mater.* **2025**, *9*, 094801. [CrossRef]
5. Jin, C.Q.; Puzniak, R.; Zhao, Z.X.; Wu, X.J.; Tatsuski, T.; Tamura, T.; Adachi, S.; Tanabe, K.; Yamauchi, H.; Tanaka, S. High-pressure synthesis and superconducting properties of the oxychloride superconductor $(Sr,Ca)_3Cu_2O_{4+\delta}Cl_{2-y}$. *Phys. Rev. B* **2000**, *61*, 778–783. [CrossRef]
6. Malozemoff, A. Second-generation high-temperature superconductor wires for the electric power grid. *Annu. Rev. Mater. Res.* **2012**, *42*, 373–397. [CrossRef]
7. Malozemoff, A.; Fleshler, S.; Rupich, M.; Thieme, C.; Li, X.; Zhang, W.; Otto, A.; Maguire, J.; Folts, D.; Yuan, J. Progress in high temperature superconductor coated conductors and their applications. *Supercond. Sci. Technol.* **2008**, *21*, 034005. [CrossRef]
8. Ihara, H.; Tokiwa, K.; Ozawa, H.; Hirabayashi, M.; Negishi, A.; Matuhata, H.; Song, Y.S. New high-T_c superconductor family of Cu-based $Cu_{1-x}Ba_2Ca_{n-1}Cu_nO_{2n+4-\delta}$ with $T_c > 116$ K. *Jpn. J. Appl. Phys.* **1994**, *33*, L503–L506. [CrossRef]

9. Tokiwa, K.; Tanaka, Y.; Iyo, A.; Tsubaki, Y.; Tanaka, K.; Akimoto, J.; Oosawa, Y.; Terada, N.; Hirabayashi, M.; Tokumoto, M. High pressure synthesis and characterization of single crystals of $CuBa_2Ca_3Cu_4O_y$ superconductor. *Phys. C Supercond.* **1998**, *298*, 209–216. [CrossRef]
10. Tsukamoto, A.; Nakanishi, K.; Yamamoto, K.; Yamauchi, H. A novel Ba-Cu-O compound synthesized by pulsed laser deposition. *Thin Solid Film.* **1996**, *274*, 138–142. [CrossRef]
11. Ou, M.-J.; Liu, Y.; Wang, Y.; Wen, H.-H. Growth of $(Cu,C)Ba_2Ca_2Cu_3O_{9\pm\delta}$ thin films on flexible Hastelloy tapes. *Supercond. Sci. Technol.* **2025**, *38*, 035015. [CrossRef]
12. Kawashima, T.; Matsui, Y.; Takayama-Muromachi, E. New oxycarbonate superconductors $(Cu_{0.5}C_{0.5})Ba_2Ca_{n-1}Cu_nO_{2n+3}$ (n = 3, 4) prepared at high pressure. *Phys. C Supercond.* **1994**, *224*, 69–74. [CrossRef]
13. Kumakura, H.; Togano, K.; Kawashima, T.; Takayama-Muromachi, E. Critical current densities and irreversibility lines of new oxycarbonate superconductors $(Cu_{0.5}C_{0.5})Ba_2Ca_{n-1}Cu_nO_{2n+3}$ (n = 3, 4). *Phys. C Supercond.* **1994**, *226*, 222–226. [CrossRef]
14. Duan, T.; Hao, J.; Chu, H.; Wen, H.-H. Preparation and superconducting properties of the $(Cu,C)Ba_2Ca_3Cu_4O_{11+y}$ films with zero-resistance transition temperature of 96 K. *Supercond. Sci. Technol.* **2020**, *33*, 025009. [CrossRef]
15. Li, Y.; Liu, Z.; Zhu, P.; He, J.; Cai, C. High-temperature $(Cu,C)Ba_2Ca_3Cu_4O_y$ superconducting films with large irreversible fields grown on $SrLaAlO_4$ substrates by pulsed laser deposition. *Crystals* **2024**, *14*, 514. [CrossRef]
16. Zhu, P.; Chen, Y.; Fan, F.; He, J.; Tong, S.; Yang, L.; Li, Y.; Guo, Y.; Cai, C. Thickness dependence of high-temperature $(Cu,C)Ba_2Ca_3Cu_4O_y$ superconducting films with large irreversible field. *ACS Appl. Electron. Mater.* **2024**, *6*, 7154–7161. [CrossRef]
17. Heine, K.; Tenbrink, J.; Thöner, M. High-field critical current densities in $Bi_2Sr_2Ca_1Cu_2O_{8+x}$/Ag wires. *Appl. Phys. Lett.* **1989**, *55*, 2441–2443. [CrossRef]
18. Balachandran, U.; Iyer, A.; Haldar, P.; Motowidlo, L. The powder-in-tube processing and properties of Bi-2223. *JOM* **1993**, *45*, 54–57. [CrossRef]
19. Toby, B.H. EXPGUI, a graphical user interface for GSAS. *J. Appl. Crystallogr.* **2001**, *34*, 210–213. [CrossRef]
20. Zhang, X.; Zhao, J.; Zhao, H.; Shi, L.; Deng, S.; Chen, J.; He, L.; Hu, Z.; Jin, C.; Zhu, J. Atomic origin of the coexistence of high critical current density and high T_c in $CuBa_2Ca_3Cu_4O_{10+\delta}$ superconductors. *NPG Asia Mater.* **2022**, *14*, 50. [CrossRef]
21. Hirai, M.; Iyo, A.; Kodama, Y.; Sundaresan, A.; Arai, J.; Tanaka, Y. Anomalous behaviour of irreversibility lines in multi-layered superconductor (Cu,C) $Ba_2Ca_3Cu_4O_y$. *Supercond. Sci. Technol.* **2004**, *17*, 423. [CrossRef]
22. Cava, R.; Batlogg, B.; Chen, C.H.; Rietman, E.; Zahurak, S.; Werder, D. Single-phase 60 K bulk superconductor in annealed $Ba_2YCu_3O_{7-\delta}$ $(0.3 < \delta < 0.4)$ with correlated oxygen vacancies in the Cu-O chains. *Phys. Rev. B* **1987**, *36*, 5719.
23. Cava, R.J.; Batlogg, B.; Sunshine, S.A.; Siegrist, T.; Fleming, R.M.; Rabe, K.; Schneemeyer, L.F.; Murphy, D.W.; Dover, R.B.V.; Gallagher, P.K. Studies of oxygen-deficient $Ba_2YCu_3O_{7-\delta}$ and superconductivity Bi(Pb)SrCaCuO. *Phys. C Supercond.* **1988**, *153–155*, 560–565. [CrossRef]
24. Jin, C.Q.; Wu, X.J.; Laffez, P.; Tatsuki, T.; Tamura, T.; Adachi, S.; Yamauchi, H.; Koshizuka, N.; Tanaka, S. Superconductivity at 80 K in $(Sr,Ca)_3Cu_2O_{4+\delta}Cl_{2-y}$ induced by apical oxygen doping. *Nature* **1995**, *375*, 301–303. [CrossRef]
25. Ito, T.; Suematsu, H.; Isawa, K.; Karppinen, M.; Yamauchi, H. Optimization of the synthesis and tuning the oxygen content of the $CuBa_2Ca_2Cu_3O_{8+\delta}$ (Cu-1223: P) superconductor. *Phys. C Supercond.* **1998**, *308*, 9–15. [CrossRef]
26. Hirai, M.; Kodama, Y.; Kito, H.; Tanaka, Y.; Tokiwa, K.; Watanabe, T.; Iyo, A. Unconventional Variation of T_c in the Multilayered Cuprate Superconductor (Cu,C) $Ba_2Ca_4Cu_5O_y$. *J. Phys. Soc. Jpn.* **2007**, *76*, 054701. [CrossRef]
27. Guo, W.; Zou, G.; Wu, A.; Wang, Y.; Bai, H.; Ren, J. Study of air heat treatment on Bi-2223/Ag superconducting tapes. *Phys. C Supercond.* **2009**, *469*, 778–781. [CrossRef]
28. Akimoto, J.; Oosawa, Y.; Tokiwa, K.; Hirabayashi, M.; Ihara, H. Crystal structure analysis of $Cu_{0.6}Ba_2Ca_3Cu_4O_{10.8}$ by single-crystal X-ray diffraction method. *Phys. C Supercond.* **1995**, *242*, 360–364. [CrossRef]